RSC Advances

PAPER

View Article Online
View Journal | View Issue

Cite this: *RSC Adv.*, 2023, **13**, 28658

Hemiaminal dynamic covalent networks with rapid stress relaxation, reprocessability and degradability endowed by the synergy of disulfide and hemiaminal bonds†

Siyao Zhu,‡[ab] Yan Wang,‡[c] Jiaxin Qin,[ab] Li Chen,[ab] Liying Zhang,[a] Yi Wei *[a] and Wanshuang Liu *[a]

Received 10th August 2023
Accepted 22nd September 2023

DOI: 10.1039/d3ra05413f

rsc.li/rsc-advances

This work proposes a strategy to address the challenge of achieving rapid reprocessability of vitrimers at mild temperatures by introducing dynamic disulfide and hemiaminal bonds into hemiaminal dynamic covalent networks (HDCNs). The resulting HDCNs, termed HDCNs-DTDA, were prepared through a facile polycondensation between formaldehyde and 4,4′-dithiodianiline. The dual dynamic bond system in the HDCNs-DTDA enables rapid stress relaxation under mild temperature (65 °C for 54 s), which is significantly faster than that observed in HDCNs containing a single dynamic bond (HDCNs-DDM). The HDCNs-DTDA also exhibit a glass transition temperature of 96 °C, excellent solvent resistance and high recovery rates (97%) of tensile strength after reprocessing. In addition, HDCNs-DTDA can be easily degraded in HCl and thiol solutions at room temperature to enable chemical recyclability. Finally, HDCNs-DTDA demonstrates fast shape memory behaviors using thermal stimulation.

Introduction

Polymeric materials, such as rubber, plastics and synthetic fibers, have been widely used in society since their invention.[1] Among them, thermosets are a promising category of polymeric materials due to their outstanding mechanical strength, excellent electrical insulation, remarkable dimensional and heating stability, and good chemical resistance.[2] They have found diverse applications in sectors such as insulating materials, coatings, encapsulants, adhesives, and composite materials.[3] However, the irreversible cross-linked networks of conventional thermosets make them difficult to recycle, which reduces their service time and causes environmental pollution.[4] In contrast, thermoplastic polymers can be easily recycled due to their ability to be altered into a flowing liquid state at high temperatures.[5] Nevertheless, the complex properties including the mechanical properties and chemical resistance properties of thermoplastic polymers are often inferior to those of thermosets.[6] To overcome this limitation, there is a need to develop novel polymeric materials that combine the advantages of thermosets and thermoplastics, such as good mechanical properties and chemical resistance, as well as reprocessability and recyclability.

In recent years, there has been increasing interest in incorporating dynamic covalent bonds into thermosets to create materials known as vitrimers or covalent adaptable networks (CANs).[7,8] These materials can offer superior reprocessability, recyclability, and degradability without compromising the advantages of traditional thermosets due to the dynamic exchange and breakage of dynamic covalent bonds in cross-linked networks under various external stimuli including high temperature, light and pH *etc.*[9–11] To data, researchers have explored various types of dynamic covalent systems for CANs, such as imine exchange,[12,13] acetal,[14,15] disulfides,[16,17] siloxane equilibration,[18,19] transesterification,[20–22] borate ester,[23,24] C–C bond exchange,[25] hindered urea bonds[26] and olefin metathesis.[27] Although great progress has been obtained for CANs, achieving rapid reprocessability under mild conditions without compromising material performance remains a challenge. Generally, high temperatures and long processing times can lead to energy consumption and degradation of the cross-linked network. To address this issue, two main approaches have been explored: regulation of the catalyst system (such as categories, concentration, and compatibility of the catalyst) and regulation

[a]*Shanghai High Performance Fibers and Composites Center (Province-Ministry Joint), Shanghai Key Laboratory of Lightweight Composite, Center for Civil Aviation Composites, Donghua University, 2999 North Renmin Road, Shanghai, China. E-mail: weiy@dhu.edu.cn; wsliu@dhu.edu.cn*

[b]*Key Laboratory of Textile Science &Technology, Ministry of Education, College of Textiles, Donghua University, 2999 North Renmin Road, Shanghai, 201620, China*

[c]*College of Materials Science & Engineering, Donghua University, 2999 North Renmin Road, Shanghai, 201620, China*

† Electronic supplementary information (ESI) available. See DOI: https://doi.org/10.1039/d3ra05413f

‡ Siyao Zhu and Yan Wang contributed equally to this work and should be considered as joint-first authors.

of the polymer structure (such as the concentration of dynamic units, structure, and content of the cross-linker).[21,22,28–30] Several studies have explored the impact of these approaches on CANs. For instance, Li *et al.*[31] prepared a dynamic epoxy vitrimer containing a catalyst of ZnAl-layered double metal hydroxide (ZnAl-LDH), which can achieve fast stress relaxation with increasing ZnAl-LDH. However, the temperature (190 °C) of stress relaxation was high. In addition, Liu *et al.*[32] obtained imine bond-crosslinked elastomeric vitrimers achieving fast stress relaxation by reducing the crosslinking degree of vitrimers. However, this led to poor mechanical properties in vitrimers with lower crosslinking degrees. Recently, a novel strategy has been proposed for achieving faster reprocessability and stress relaxation in CANs by incorporating dual dynamic covalent bonds.[33,34] For example, Yang *et al.*[35] developed a polyurethane material based on disulfide bonds and carbamate groups, which exhibited fast stress relaxation at moderate temperatures.

Polyhexahydrotriazines (PHT), a highly cross-linked network, were first reported by Hedrick and coworkers through the polymerization of bis(aniline) and formaldehyde at high temperature and exhibit good mechanical properties and acidic degradation.[36] However, PHT does not contain dynamic covalent bonds and thus cannot be reprocessed. As the precursors of PHT, hemiaminal dynamic covalent networks (HDCNs) can be reprocessed, self-healed and degraded under acidic conditions. In this study, we developed novel HDCNs with high reprocessing efficiency under mild conditions and versatile degradability by simultaneously introducing disulfide and hemiaminal dynamic bonds into their crosslinked networks. The structural dynamic behaviors, reprocessability and degradability of the prepared HDCNs were investigated and compared with their counterparts that only contained the hemiaminal dynamic bond. In addition to the thermal and mechanical properties, the shape memory behavior of the prepared HDCNs was also demonstrated.

Experimental

Materials

Paraformaldehyde (PFA, ≥99.8%), *N*-methyl-2-pyrrolidone (NMP, ≥99.5%), acetone (≥99.5%), anhydrous ethanol (≥99.5%), tetrahydrofuran (THF, ≥99.5%), *N*,*N*-dimethylformamide (DMF, 99.5%), chloroform ($CHCl_3$, ≥99%) hydrochloric acid (HCl, 36%), and sodium hydroxide (NaOH, ≥96%) were obtained from Sinopharm Chemical Reagent Co., Ltd., Shanghai, China. 2-Mercaptoethanol (≥99%), 4,4′-dithiodianiline (DTDA, ≥98%) and 4,4′-methylenedianiline (DDM, ≥98%) were purchased from Shanghai Taitan Technology Co., Ltd., Shanghai, China. All of the chemicals were utilized as received without further purification.

Preparation of HDCNs-DTDA

PFA (3.8 g), distilled water (6.0 mL) and NMP (54.0 mL) were added to a flask at room temperature and stirred at 80 °C for 2 h. After the transparent solution was cooled to 50 °C, DTDA (12.5 g) was added and stirred homogenously for 1 h. Later, the prepolymer solution was poured into a polytetrafluoroethylene mold and staged heated to 50 °C for 6 h, 80 °C for 2 h, and 110 °C for 2 h. Then, the prepolymer was ground to a fine powder and placed into the rectangular steel punch molds. The molds were pressed at 110 °C under 0.3 MPa for 30 min. After cooling to the ambient temperature, the HDCNs-DTDA samples were obtained by demolding and polishing for various measurements. The above preparation processes are illustrated in Scheme 1a and b.

Preparation of HDCNs-DDM

HDCNs-DDM was prepared by the same procedure as that of HDCNs-DTDA by using DDM instead of DTDA (Scheme 1 c).

Reprocessing of HDCNs

A hot-press treatment was used to perform the reprocessing tests. The HDCNs were ground to a fine powder and pressed at 130 °C under a pressure of 6 MPa for 5–30 min. After cooling to ambient temperature, the reprocessed samples were collected.

Chemical degradation of HDCNs-DTDA

Approximately 300 mg of HDCNs-DTDA was placed in 15 mL of 2-mercaptoethanol/*N*,*N*-dimethylformamide (0.1 M) at room temperature. The sample was removed from the solutions and weighed after drying. The percentage of residual weight was calculated according to the residual weight. In addition, approximately 25 mg of the HDCNs-DTDA fragments were immersed into 15 mL of 0.1 M HCl solution in different organic solvent solutions at ambient temperature. Degradation times were recorded when the samples were completely dissolved in the solution.

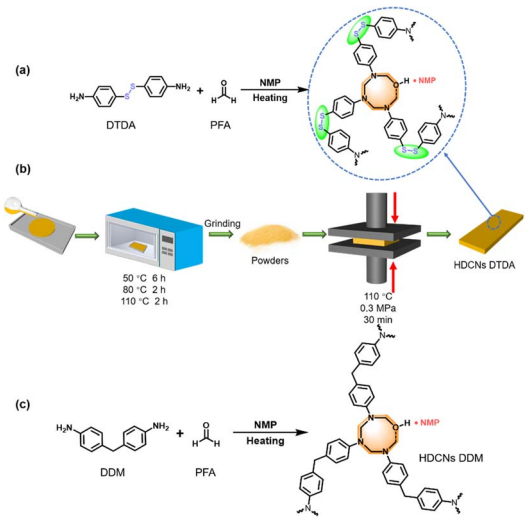

Scheme 1 (a) Synthetic route of HDCNs DTDA from DTDA and PFA. (b) Preparation procedures of HDCNs DTDA. (c) Synthetic route of HDCNs from DDM and PFA.

Shape memory behavior of HDCNs-DTDA

The HDCNs-DTDA film was cut into rectangular and triangular shapes. The samples were temporarily deformed at 110 °C by external force for seconds and retained their shapes at room temperature. These samples were then heated at 110 °C to recover their original shapes.

Characterization

Fourier transform infrared spectra (FTIR) were obtained using a Nicolet 6700 FTIR spectrometer, and 32 scans were recorded from 4000 to 450 cm^{-1} range using the attenuated total reflection (ATR) mode. The solid state ^{13}C NMR measurement was conducted on a Bruker Advance 400 spectrometer. The dynamic mechanical properties were assessed using a TA Instruments DMA Q800 equipped with a tensile clamp. Samples with dimensions of 25 × 6 × 0.5 mm^3 were scanned at a heating rate of 3 °C, frequency of 1 Hz and oscillating amplitude of 15 μm. Stress relaxation experiments were also carried out on a TA Instruments DMA Q800 using the tensile mode. The rectangular specimens (25 × 6 × 0.5 mm^3) of the sample were first equilibrated at the preset temperature for 10 min and then applied to a constant strain of 1.0%. The development of the relaxation modulus value was recorded over time. Tensile testing was measured using a Wance ETM104B-EX electronic universal testing machine. The samples had dimensions of 40 mm (length) × 6 mm (width) × 0.5 mm (thickness) at a crosshead speed of 2 mm min^{-1}. All data were based on three effective testing results.

Results and discussion

Preparation and chemical characterization of HDCNs

HDCNs-DTDA and HDCNs-DDM were prepared by a one-pot polycondensation between PFA and two aromatic amines (DTDA and DDM) as shown in Scheme 1a and c. The chemical structures of the two HDCNs were characterized by FTIR. The FTIR spectra of DTDA, HDCNs-DTDA, DDM and HDCNs-DDM are shown in Fig. 1. Compared with the FTIR spectrum of DTDA, the signals of primary amine at 3414 and 3334 cm^{-1} disappeared in the spectrum of HDCNs-DTDA, and the appearance of the new peak at 3329 cm^{-1} was ascribed to the hydroxyl from the hemiaminal group.[37] The new peak at 1223 cm^{-1} belongs to the C–N stretching vibration in the hemiaminal group.[38] In addition, the asymmetric and symmetric stretching vibrations of the methylene group on the hemiaminal group are observed at 2826 and 2922 cm^{-1}, respectively.[37] The peak at 1672 cm^{-1} results from the C=O stretching vibration of the residual NMP solvent in HDCNs.[39] Moreover, the characteristic peak of S–S at approximately 514 cm^{-1} is still maintained in the spectrum of HDCNs-DTDA.[38] Similar peaks are observed in the FTIR spectra of DDM and HDCNs-DDM. Moreover, solid state ^{13}C NMR was also performed for HDCNs-DTDA. As shown in Fig. S1,† the carbon signals of hemiaminal group from HDCNs-DTDA are detected at around 65 ppm. The carbon signals within the range of 100 to 150 ppm can be attributed to the aromatic carbons of HDCNs-DTDA. It should be noted that the carbon signals of HDCNs-DTDA in ^{13}C NMR were similar to those of reported HDCNs.[40]

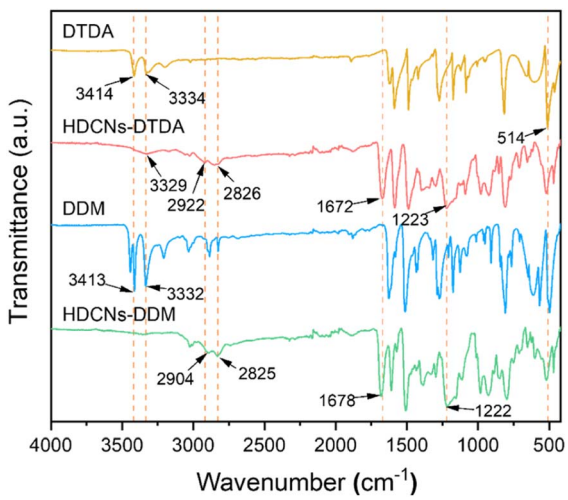

Fig. 1 FTIR spectra of DTDA, HDCNs-DTDA, DDM and HDCNs-DDM.

Stress relaxation

The dynamic response of HDCNs-DDM and HDCNs-DTDA was characterized by temperature-dependent stress relaxation experiments. The normalized relaxation modulus was measured as a function of relaxation time at different temperatures (Fig. 2a and b). The relaxation moduli of both HDCNs decrease over time at all temperatures, which is consistent with the Maxwell model. The relaxation time (τ) is commonly defined as the time when the modulus is reduced to $1/e$ (~37%) of the initial modulus ($G/G_0 = 1/e$).[41] These two HDCNs show quite different stress relaxation behaviors. The τ values of HDCNs-DTDA are much lower than those of HDCNs-DDM at the same test temperature. Representatively, the τ values of HDCNs-DTDA and HDCNs-DDM are 124 and 512 s at 60 °C, respectively. The fast relaxation behavior of HDCNs-DTDA can be attributed to its dual dynamic network, which results in fast topology rearrangements through the reversible exchange reactions between dynamic covalent bonds. Furthermore, the relationship between τ and test temperature (T) follows the Arrhenius equation, as shown in eqn (1).[11]

$$\tau(T) = \tau_0 \exp\left(\frac{E_a}{RT}\right) \quad (1)$$

where τ_0 is the characteristic relaxation time at infinite temperature, τ is the relaxation time, R is the universal gas constant (8.31 J mol^{-1} K^{-1}) and E_a is the activation energy. The calculated E_a values for HDCNs-DTDA and HDCNs-DDM are 80 and 131 kJ mol^{-1}, respectively. In accordance with eqn (1), the physical parameters suggest that the activation energy, E_a, primarily characterizes the responsiveness of the relaxation velocity to temperature variations rather than representing the activation energy of exchange reactions involving acetal bonds.[42]

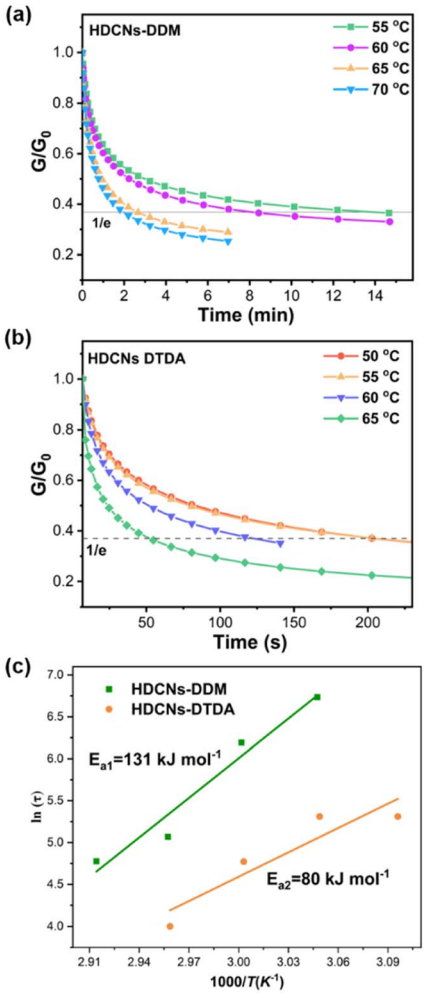

Fig. 2 Stress relaxation of HDCNs-DDM (a) and HDCNs-DTDA (b) at different temperatures. Arrhenius fitted line of the characteristic relaxation time τ *versus* 1000/T for HDCNs (c).

The topology freezing transition temperature (T_v) is another crucial parameter for HDCNs due to the temperature-dependent behavior of topology network rearrangement in bond exchange reactions. Typically, T_v is defined as the temperature where the viscosity of materials reaches 10^{12} Pa s[15]. When the temperature is above T_v, vitrimer materials undergo a transition from a solid-like state to a viscoelastic liquid state.[43] The τ at T_v can be determined according to eqn (2).[30]

$$\eta = \frac{1}{3}E'\tau \quad (2)$$

where η is the viscosity (10^{12} Pa s) at T_v and E' is the equilibrium value of storage modulus in the rubbery region from DMA tests. The obtained τ at T_v was utilized in the Arrhenius' fitted line (Fig. 2c) to attain the T_v. The T_v value of HDCNs-DTDA (−6.8 °C) is much lower than that of HDCNs-DDM (25.4 °C), which can explain the fast relaxation behavior of HDCNs-DTDA at relatively low temperatures compared to HDCNs-DDM.

Reprocessing of HDCNs

In general, thermoplastic polymers can be easily reprocessed using thermomechanical methods such as extrusion and injection.[44] However, conventional thermosets cannot be reprocessed through thermomechanical methods due to their permanent crosslinked networks. Owing to the introduction of dynamic disulfide and/or hemiaminal bonds, two HDCNs can be reprocessed by hot pressing under 6 MPa pressure at 130 °C (Fig. 3a). Fig. 3b and c present the representative stress–strain curves of HDCNs-DDM and HDCNs-DTDA with different processing times. Compared with HDCNs-DTDA (38.5 MPa), the original HDCNs-DDM has a higher tensile strength (56.2 MPa), as shown in Table 1. The reprocessed HDCNs-DTDA can reach a high retention rate (97%) of tensile strength with a shorter processing time (10 min). In contrast, HDCNs-DDM need 30 min to obtain a 91% retention rate for tensile strength. The enhanced reprocessing efficiency of HDCNs-DTDA can be attributed to the incorporation of dual dynamic covalent bonds (Fig. 3d).[45,46] A comparison of HDCNs-DTDA with reported vitrimers containing single disulfide or hemiaminal bonds was made in terms of reprocessing temperature and reprocessing time, as shown in Table S1.† Among them, HDCNs-DTDA in this work has the lowest reprocessing temperature and shortest reprocessing time, which would contribute to energy savings and enhances production efficiency. In addition, all the reprocessed HDCNs samples exhibit a slightly increased tensile modulus compared with the corresponding original counterparts (Table 1).

DMA measurements were conducted to evaluate the thermomechanical properties of the original and reprocessed

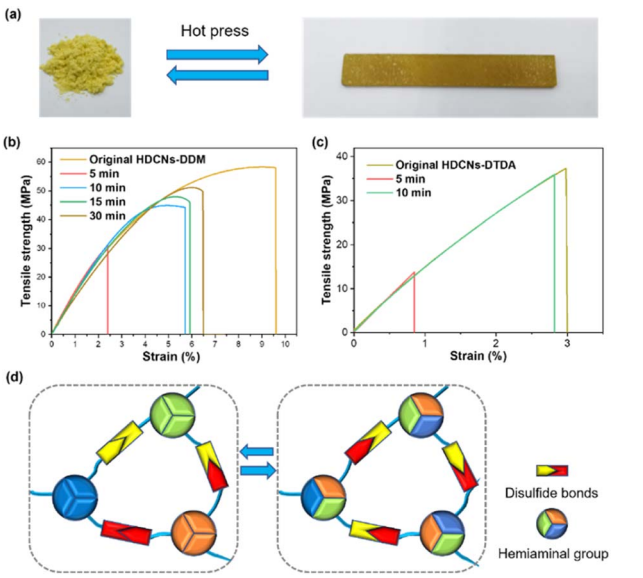

Fig. 3 Photographs of both HDCNs-DTDA before and after reprocessing treatment (a); representative tensile strength–strain curves of original and reprocessed HDCNs-DDM (b) and HDCNs-DTDA (c) with different reprocessing times. Mechanism of reversible network rearrangement for HDCNs-DTDA (d).

Table 1 Tensile properties of original and reprocessed HDCNs

Samples	Tensile strength (MPa)	Tensile modulus (MPa)	Retention of strength (%)
Original HDCNs-DDM	56.2 ± 2	1706 ± 68	—
Reprocessed-5 min	31.3 ± 1	1787 ± 74	55
Reprocessed-10 min	45.6 ± 1	1773 ± 73	80
Reprocessed-15 min	49.1 ± 1	1782 ± 53	88
Reprocessed-30 min	51.7 ± 1	1718 ± 84	91
Original HDCNs-DTDA	38.5 ± 4	1530 ± 54	—
Reprocessed-5 min	15.2 ± 1	1567 ± 60	39
Reprocessed-10 min	37.6 ± 2	1613 ± 105	97

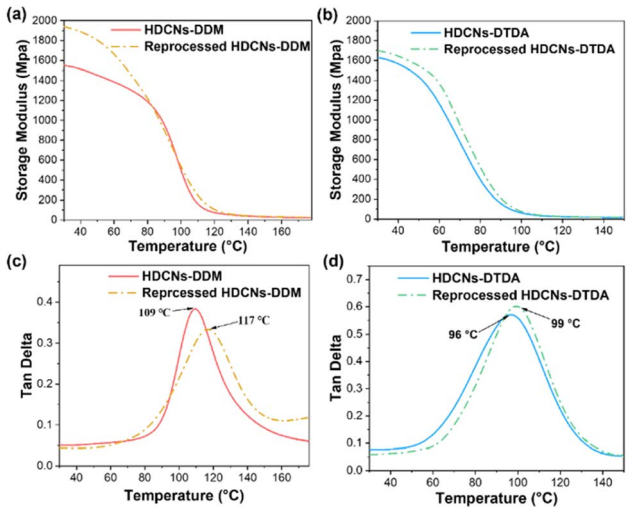

Fig. 4 Storage modulus *versus* temperature curves of original and reprocessed HDCNs-DDM (a) and HDCNs-DTDA (b). Tan δ *versus* temperature curves of original and reprocessed HDCNs-DDM (c) and HDCNs-DTDA (d).

HDCNs. The curves of storage modulus (E') and tan δ as a function of temperature are presented in Fig. 4, and the detailed data are displayed in Table 2. The storage moduli of the original HDCNs-DDM and HDCNs-DTDA at 30 °C were 1552 and 1628 MPa, respectively. This indicates that both HDCNs have acceptable rigidness as thermosetting polymers. The glass transition temperature (T_g) of the two HDCNs was determined by the peak temperature of the tan δ *versus* temperature curve. The T_g values of the original HDCNs-DDM and HDCNs-DTDA are 109 and 96 °C, respectively. After reprocessing, both HDCNs show enhanced storage modulus (30 °C) and T_g values compared with original HDCNs, especially for HDCNs-DDM (Table 2). This might be because the reprocessing treatment could be regarded as a post cure process, which would result in an increased crosslinking degree for reprocessed HDCNs. Based on rubber elasticity theory, the cross-link density (ν_e) of original and reprocessed HDCNs was calculated according to eqn (3).[11]

$$\nu_e = \frac{E'}{3RT} \quad (3)$$

where R is the gas constant, E' is the storage modulus of HDCNs at T_g + 50 °C, and T is the absolute temperature of the T_g + 50 °C. As shown in Table 2, both reprocessed HDCNs show increased cross-link density compared with the original HDCNs. This indicates that the reprocessing treatment does not deteriorate the thermal–mechanical properties of the two HDCNs.

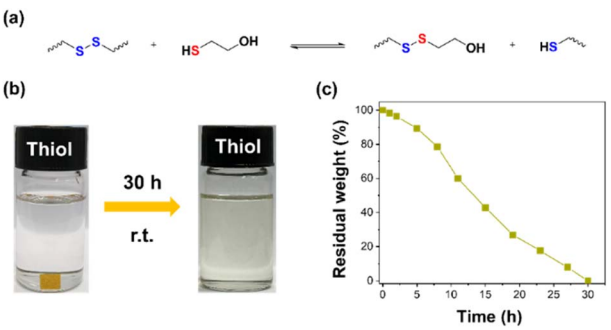

Fig. 5 Thiol–disulfide bond exchange reaction between HDCNs-DTDA and 2-mercaptoethanol (a); chemical degradation of HDCN-DTDA in the 2-mercaptoethanol/DMF solution. (b) Percentage of residual weight of HDCNs-DTDA as a function of time in the 2-mercaptoethanol/DMF solution (c).

Table 2 Thermophysical properties of pristine and reprocessed HDCNs

Samples	E' at 30 °C (MPa)	T_g (°C)	E' at T_g + 50 °C (MPa)	ν_e (mol m^{-3})
HDCNs DDM	1552	109	28	7060
Reprocessed HDCNs DDM	1938	117	30	7202
HDCNs DTDA	1628	96	18	4843
Reprocessed HDCNs DTDA	1696	99	20	5492

Chemical degradability and stability

In recent decades, developing degradable thermosetting polymers has drawn increasing attention owing to the increasing concerns about environmental protection and energy conservation. Introducing degradable linkages is a well-established method to endow thermosetting polymers with chemical degradability.[3] It has been reported that the disulfide bonds can break in the thiol solution due to the thiol–disulfide bond exchange reaction (Fig. 5a),[9,47,48] and the hemiaminal networks can degrade in the aqueous acid solution due to the breaking of hemiaminal dynamic bonds.[36] Based on the above chemical principles, HDCNs-DTDA was immersed in the 2-mercaptoethanol and HCl solutions to confirm its chemical degradability. As shown in Fig. 5b and c, a fragment of HDCNs-DTDA can be gradually dissolved in the thiol/DMF solution at ambient temperature within 30 h. In addition, HDCNs-DTDA can also chemically degrade in 0.1 M HCl solutions containing different organic solvents (Fig. 6a). In contrast, HDCNs-DTDA is insoluble in aqueous HCl solution. This can be attributed to the poor wettability of the aqueous acid solution toward HDCNs-DTDA.[49] Compared with degradation in HCl/THF (24 h) and HCl/acetone (28 h), the HDCNs-DTDA sample shows a much shorter degradation time (3 h) in the HCl/ethanol solution (Fig. 6b). The above results indicate that organic solvents have a significant impact on the degradation behavior of HDCNs-DTDA in the acidic solution. Compared with vitrimers containing single disulfide or hemiaminal bonds (Table S1†), HDCNs-DTDA has optional degradation conditions (acid or thiol solution) in practical applications.

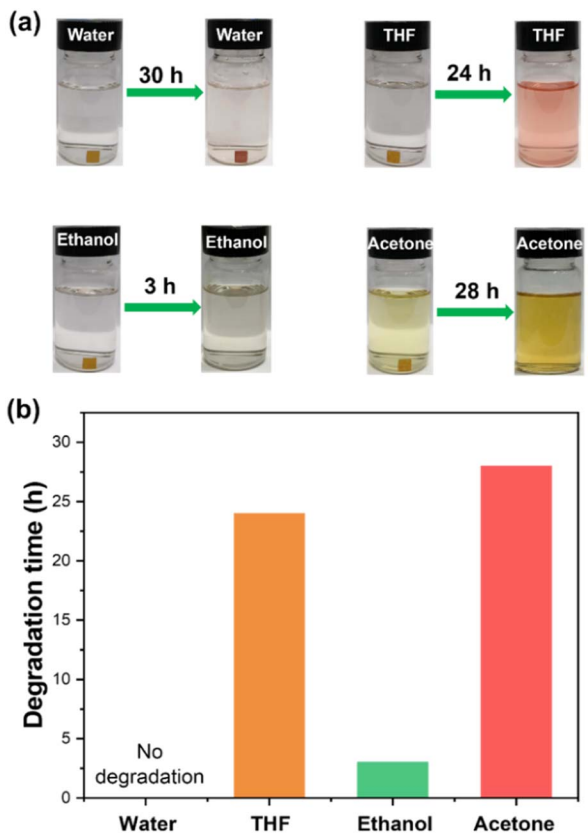

Fig. 6 Chemical degradation (a) and degradation time (b) of HDCNs-DTDA in HCl solutions containing different organic solvents.

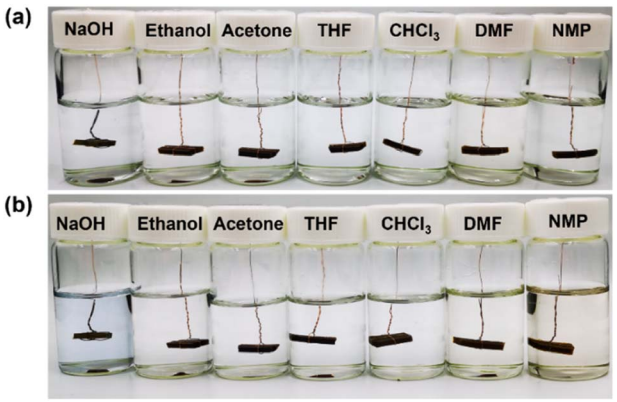

Fig. 7 Photographs of the HDCNs-DTDA samples in different solvents (a) before and (b) after staying for 120 h at ambient temperature.

Assessing the chemical resistance of HDCNs-DTDA is very important due to the incorporation of disulfide and hemiaminal groups. Herein, many HDCNs-DTDA samples were submerged in different solvents, including NaOH solution (1 M), ethanol, acetone, THF, chloroform, DMF and NMP at ambient temperature for 120 h. As presented in Fig. 7, HDCNs-DTDA demonstrates excellent chemical resistance in these solutions. Almost no changes in the sample appearance and solvent color were observed. This reveals that HDCNs-DTDA can be used like traditional thermosets in many fields and only degrade under specific chemical stimuli.

Shape memory behavior

HDCNs-DTDA is expected to have thermally induced shape memory behavior because of its viscoelastic characteristics as investigated by DMA. As shown in Fig. 8, the rectangular and

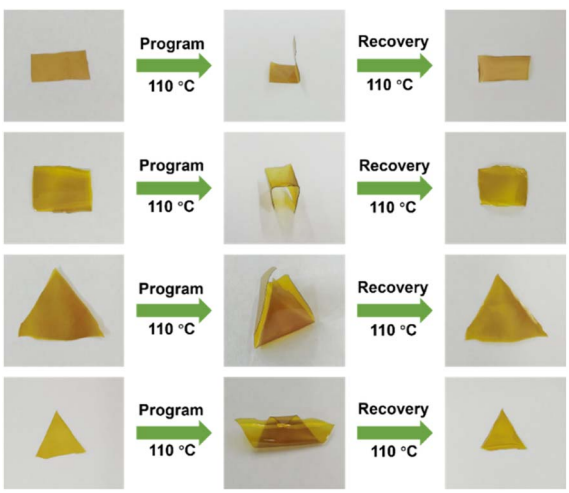

Fig. 8 Photographs of the thermally induced shape memory behavior of HDCNs-DTDA with different original shapes.

triangular HDCNs-DTDA samples were first deformed into shapes of "L", "U", cone and crimp at 110 °C (above T_g). Subsequently, the samples were immediately cooled to room temperature to fix their deformed shapes. When the samples were reheated to 110 °C, all the samples recovered to their initial shapes. These observations verify the shape memory behavior of HDCNs-DTDA, and the relevant mechanism can be explained as follows. As the temperature rises above the T_g of HDCNs, chain segment motion and exchange reactions between dynamic covalent bonds are activated, allowing the external force to deform its shape.[50] When the temperature decreases to room temperature, the chain segment is immobilized which fixes the temporarily deformed shape. After reheating to a temperature above the T_g of HDCNs-DTDA, the potential energy can be released from crosslinked networks, allowing HDCNs-DTDA to recover its original shape. Such functional characteristics make shape memory polymers a promising candidate for various applications, such as biomedicine, aerospace, electronic components, and soft robots.[51]

Conclusions

In summary, this study successfully developed a recyclable thermoset, HDCNs-DTDA, which contains dual dynamic covalent bonds through a polycondensation reaction between formaldehyde and 4,4′-dithiodianilin. Compared with HDCNs-DDM (only containing dynamic hemiaminal groups), the prepared HDCNs-DTDA exhibit a much faster stress relaxation rate and shorter reprocessing time. The HDCNs-DTDA can be rapidly reprocessed in 10 min at 130 °C under 6 MPa, which is attributed to the rapid bond exchange reactions from dual dynamic bonds. The thermal and mechanical properties of HDCNs-DTDA are well retained after reprocessing. In particular, the retention rate of tensile strength of reprocessed HDCNs-DTDA can reach nearly 97%. The HDCNs-DTDA can be easily degraded in the acidic or thiol solutions at room temperature, but shows outstanding resistance to many common organic solvents, such as conventional thermosets. Finally, the HDCNs-DTDA also displays good shape memory behaviors above its T_g. Given its easy synthesis and recycling ability, HDCNs-DTDA has great potential for use in coating and composite applications.

Author contributions

Siyao Zhu: investigation; data curation; writing – original draft. Yan Wang: investigation; data curation; writing – original draft. Jiaxin Qin: investigation. Li Chen: investigation; data curation. Liying Zhang: resources; writing – review & editing. Yi Wei: resources; supervision; writing – review & editing. Wanshuang Liu: conceptualization; supervision; writing – review & editing.

Conflicts of interest

The authors declare no competing financial interest.

Acknowledgements

This work was supported by Shanghai Pujiang Program (21PJ1423400) and Shanghai Key Laboratory of Lightweight Composite (2232020A4-10).

References

1 K. Wang, K. Amin, Z. An, Z. Cai, H. Chen, H. Chen, Y. Dong, X. Feng, W. Fu, J. Gu, Y. Han, D. Hu, R. Hu, D. Huang, F. Huang, F. Huang, Y. Huang, J. Jin, X. Jin, Q. Li, T. Li, Z. Li, Z. Li, J. Liu, J. Liu, S. Liu, H. Peng, A. Qin, X. Qing, Y. Shen, J. Shi, X. Sun, B. Tong, B. Wang, H. Wang, L. Wang, S. Wang, Z. Wei, T. Xie, C. Xu, H. Xu, Z.-K. Xu, B. Yang, Y. Yu, X. Zeng, X. Zhan, G. Zhang, J. Zhang, M. Q. Zhang, X.-Z. Zhang, X. Zhang, Y. Zhang, Y. Zhang, C. Zhao, W. Zhao, Y. Zhou, Z. Zhou, J. Zhu, X. Zhu and B. Z. Tang, *Mater. Chem. Front.*, 2020, **4**, 1803–1915.
2 Y. Yang, Y. Xu, Y. Ji and Y. Wei, *Prog. Mater. Sci.*, 2021, **120**, 100710.
3 S. Ma and D. C. Webster, *Prog. Polym. Sci.*, 2018, **76**, 65–110.
4 S. Wang, S. Ma, Q. Li, X. Xu, B. Wang, K. Huang, Y. liu and J. Zhu, *Macromolecules*, 2020, **53**, 2919–2931.
5 H. Lei, S. Wang, D. J. Liaw, Y. Cheng, X. Yang, J. Tan, X. Chen, J. Gu and Y. Zhang, *ACS Macro Lett.*, 2019, **8**, 582–587.
6 Y. Yang, L. Huang, R. Wu, W. Fan, Q. Dai, J. He and C. Bai, *ACS Appl. Mater. Interfaces*, 2020, **12**, 33305–33314.
7 D. Montarnal, M. Capelot, F. Tournilhac and L. Leibler, *Science*, 2011, **334**, 965–968.
8 L. Zhong, Y. Hao, J. Zhang, F. Wei, T. Li, M. Miao and D. Zhang, *Macromolecules*, 2022, **55**, 595–607.
9 M. Podgórski, B. D. Fairbanks, B. E. Kirkpatrick, M. McBride, A. Martinez, A. Dobson, N. J. Bongiardina and C. N. Bowman, *Adv. Mater.*, 2020, **32**, 1906876.
10 Z. Wang, M. Yang, X. Wang, G. Fei, Z. Zheng and H. Xia, *J. Mater. Chem. A*, 2020, **8**, 25047–25052.
11 Q. Li, S. Ma, P. Li, B. Wang, Z. Yu, H. Feng, Y. Liu and J. Zhu, *Macromolecules*, 2021, **54**, 8423–8434.
12 P. Zamani, O. Zabihi, M. Ahmadi, R. Mahmoodi, T. Kannangara, P. Joseph and M. Naebe, *ACS Sustainable Chem. Eng.*, 2021, **10**, 1059–1069.
13 X. He, X. Shi, C. Chung, Z. Lei, W. Zhang and K. Yu, *Composites, Part B*, 2021, **221**, 109004.
14 Q. Li, S. Ma, P. Li, B. Wang, H. Feng, N. Lu, S. Wang, Y. Liu, X. Xu and J. Zhu, *Macromolecules*, 2021, **54**, 1742–1753.
15 Q. Li, S. Ma, S. Wang, Y. Liu, M. Abu Taher, B. Wang, K. Huang, X. Xu, Y. Han and J. Zhu, *Macromolecules*, 2020, **53**, 1474–1485.
16 M. Zheng, Q. Guo, X. Yin, N. N. Getangama, J. R. de Bruyn, J. Xiao, Y. Bai, M. Liu and J. Yang, *J. Mater. Chem. A*, 2021, **9**, 6981–6992.
17 S. Zhao, D. Wang and T. P. Russell, *ACS Sustainable Chem. Eng.*, 2021, **9**, 11091–11099.
18 S. Wu, Z. Yang, S. Fang, Z. Tang, F. Liu and B. Guo, *J. Mater. Chem. A*, 2019, **7**, 1459–1467.
19 Q. Liu, L. Jiang, Y. Zhao, Y. Wang and J. Lei, *Macromol. Chem. Phys.*, 2019, **220**, 1900149.

20 W. Zhang, J. Wu, L. Gao, B. Zhang, J. Jiang and J. Hu, *Green Chem.*, 2021, **23**, 2763–2772.
21 L. Yue, M. Amirkhosravi, K. Ke, T. G. Gray and I. Manas-Zloczower, *ACS Appl. Mater. Interfaces*, 2021, **13**, 3419–3425.
22 Y. Xu, S. Dai, H. Zhang, L. Bi, J. Jiang and Y. Chen, *ACS Sustainable Chem. Eng.*, 2021, **9**, 16281–16290.
23 C. Zhang, X. Wang, D. Liang, H. Deng, Z. Lin, P. Feng and Q. Wang, *J. Mater. Chem. A*, 2021, **9**, 18431–18439.
24 L. Xie, Y. Wang, G. Chen, H. Feng, N. Zheng, H. Ren, Q. Zhao and T. Xie, *Compos. Commun.*, 2021, **28**, 100979.
25 Z. P. Zhang, M. Z. Rong and M. Q. Zhang, *Adv. Funct. Mater.*, 2018, **28**, 1706050.
26 J. Zhang, C. Zhang, F. Song, Q. Shang, Y. Hu, P. Jia, C. Liu, L. Hu, G. Zhu, J. Huang and Y. Zhou, *Chem. Eng. J.*, 2022, **429**, 131848.
27 Y.-X. Lu, F. Tournilhac, L. Leibler and Z. Guan, *J. Am. Chem. Soc.*, 2012, **134**, 8424–8427.
28 C. Hao, T. Liu, S. Zhang, W. Liu, Y. Shan and J. Zhang, *Macromolecules*, 2020, **53**, 3110–3118.
29 J. Shi, T. Zheng, Y. Zhang, B. Guo and J. Xu, *Polym. Chem.*, 2021, **12**, 2421–2432.
30 H. Memon, H. Liu, M. A. Rashid, L. Chen, Q. Jiang, L. Zhang, Y. Wei, W. Liu and Y. Qiu, *Macromolecules*, 2020, **53**, 621–630.
31 G. Li, P. Zhang, S. Huo, Y. Fu, L. Chen, Y. Wu, Y. Zhang, M. Chen, X. Zhao and P. Song, *ACS Sustainable Chem. Eng.*, 2021, **9**, 2580–2590.
32 Y. Liu, Z. Tang, J. Chen, J. Xiong, D. Wang, S. Wang, S. Wu and B. Guo, *Polym. Chem.*, 2020, **11**, 1348–1355.
33 Y. Yang, L. Huang, R. Wu, Z. Niu, W. Fan, Q. Dai, L. Cui, J. He and C. Bai, *ACS Appl. Mater. Interfaces*, 2022, **14**, 3344–3355.
34 M. Chen, L. Zhou, Y. Wu, X. Zhao and Y. Zhang, *ACS Macro Lett.*, 2019, **8**, 255–260.
35 X. Yang, S. Wang, X. Liu, Z. Huang, X. Huang, X. Xu, H. Liu, D. Wang and S. Shang, *Green Chem.*, 2021, **23**, 6349–6355.
36 J. M. Garcia, G. O. Jones, K. Virwani, B. D. McCloskey, D. J. Boday, G. M. ter Huurne, H. W. Horn, D. J. Coady, A. M. Bintaleb, A. M. S. Alabdulrahman, F. Alsewailem, H. A. A. Almegren and J. L. Hedrick, *Science*, 2014, **344**, 732–735.
37 Z. Yang, C. Duan, Y. Sun, T. Wang, X. Zhang and Q. Wang, *Ind. Eng. Chem. Res.*, 2019, **58**, 10599–10608.
38 L. Chen, S. Zhu, I. Toendepi, Q. Jiang, Y. Wei, Y. Qiu and W. Liu, *Polymers*, 2020, **12**, 2375.
39 Y. C. Yuan, Y. X. Sun, S. J. Yan, J. Q. Zhao, S. M. Liu, M. Q. Zhang, X. X. Zheng and L. Jia, *Nat. Commun.*, 2017, **8**, 14657.
40 J. M. García, G. O. Jones, K. Virwani, B. D. McCloskey, D. J. Boday, G. M. ter Huurne, H. W. Horn, D. J. Coady, A. M. Bintaleb, A. M. S. Alabdulrahman, F. Alsewailem, H. A. A. Almegren and J. L. Hedrick, *Science*, 2014, **344**, 732–735.
41 S. Wang, S. Ma, Q. Li, X. Xu, B. Wang, W. Yuan, S. Zhou, S. You and J. Zhu, *Green Chem.*, 2019, **21**, 1484–1497.
42 M. Chen, H. Si, H. Zhang, L. Zhou, Y. Wu, L. Song, M. Kang and X.-L. Zhao, *Macromolecules*, 2021, **54**, 10110–10117.
43 Z. Xiang, C. Chu, H. Xie, T. Xiang and S. Zhou, *ACS Appl. Mater. Interfaces*, 2021, **13**, 1463–1473.
44 S. Kakadellis and G. Rosetto, *Science*, 2021, **373**, 49–50.
45 S. Nevejans, N. Ballard, J. I. Miranda, B. Reck and J. M. Asua, *Phys. Chem. Chem. Phys.*, 2016, **18**, 27577–27583.
46 C. H. Fox, G. M. ter Hurrne, R. J. Wojtecki, G. O. Jones, H. W. Horn, E. W. Meijer, C. W. Frank, J. L. Hedrick and J. M. García, *Nat. Commun.*, 2015, **6**, 7417.
47 A. Ruiz de Luzuriaga, R. Martin, N. Markaide, A. Rekondo, G. Cabanero, J. Rodriguez and I. Odriozola, *Mater. Horiz.*, 2016, **3**, 241–247.
48 Y. Hao, L. Zhong, T. Li, J. Zhang and D. Zhang, *ACS Sustainable Chem. Eng.*, 2023, **11**, 11077–11087.
49 X. Xu, S. Ma, J. Wu, J. Yang, B. Wang, S. Wang, Q. Li, J. Feng, S. You and J. Zhu, *J. Mater. Chem. A*, 2019, **7**, 15420–15431.
50 Z. Li, R. Yu and B. Guo, *ACS Appl. Bio Mater.*, 2021, **4**, 5926–5943.
51 Y. Yang, L. Huang, R. Wu, W. Fan, Q. Dai, J. He and C. Bai, *ACS Appl. Mater. Interfaces*, 2020, **12**, 33305–33314.